Applied Catalysis B: Environmental 240 (2019) 102–111

Contents lists available at ScienceDirect

Applied Catalysis B: Environmental

journal homepage: www.elsevier.com/locate/apcatb

Charge transfer/mass transport competition in advanced hybrid electrocatalytic wastewater treatment: Development of a new current efficiency relation

Emmanuel Mousset[a,*], Yoan Pechaud[b,*], Nihal Oturan[b], Mehmet A. Oturan[b]

[a] Laboratoire Réactions et Génie des Procédés, Université de Lorraine, CNRS, LRGP, F-54000 Nancy, France
[b] Université Paris-Est, Laboratoire Géomatériaux et Environnement (LGE), EA 4508, UPEM, 5 bd Descartes, 77454 Marne-la-Vallée Cedex 2, France

ARTICLE INFO

Keywords:
Advanced oxidation processes
Charge transfer
Homogeneous/heterogeneous catalysis
Mass transport
Modeling

ABSTRACT

The contribution of homogeneous versus heterogeneous catalytic oxidation has been studied for the first time in a hybrid anodic oxidation (AO)/electro-Fenton (EF) batch reactor at different initial organic load in terms of chemical oxygen demand (COD) values of 1.61, 12.1 and 23.3 g-O_2 L^{-1}. The rate of three (electro)-chemical processes, e.g., (i) AO at the surface of boron-doped diamond (BDD) anode, (ii) Fenton oxidation in the bulk solution and (iii) mediated oxidation (MO) in the bulk solution, have been considered in a mathematical model. The mass transfer coefficient was depending on the concentration of the compound due to the unstationary behavior in the diffusion layer at the vicinity of the anode. After calibration and validation of the model with experimental data, it could be noticed that the competition between the mass transport and the charge transfer was evolving according to the COD load. At 1.61 g-O_2 L^{-1}, the applied current density was higher than the limiting current density all along the treatment, meaning that the process was under mass transport control. In this case, the Fenton oxidation rate had the highest contribution in the oxidation efficiency while AO oxidation rate had the lowest efficiency. Increasing the initial COD concentration up to 23.3 g-O_2 L^{-1}, made raising the influence of AO process that became predominant after a certain electrolysis time, before reaching the critical time (t_{cr}). Finally, a new current efficiency expression has been proposed by taking into account the three reaction rates and the model could fit the experimental data, showcasing a promising approach. These results further emphasized the need to adapt the reactor design to favor either AO and/or Fenton oxidation according to the organic load of wastewater to be treated, i.e., as pre-treatment or polishing treatment.

1. Introduction

Numerous hazardous contaminants, namely persistant organic pollutants (POPs), remained in the environment, especially in water bodies [1,2]. Most of these contaminants are biorecalcitrants and cannot be therefore complety removed in conventional wastewater treatment plants [3,4].

Advanced physico-chemical treatments such as advanced oxidation processes (AOPs) have been therefore developed to face this issue [5,6]. They all rely on the production of a strong oxidant, mostly hydroxyl radical ($^{\bullet}OH$) that has a very high oxidation power ($E^{\circ}(^{\bullet}OH/H_2O)$ = 2.8 V/SHE) [7,8]. This oxidant reacts especially quickly with aromatics compounds and C=C double bonds with very high rate constants (10^8-10^{10} M^{-1} s^{-1}) [9], major chemical structures present in organoxenobiotics molecules. In particular, emerging electrochemical AOPs (EAOPs) offer the advantages of producing continuously and *in situ* the $^{\bullet}OH$ radicals [10,11]. Two main ways have been considered until now to produce these $^{\bullet}OH$, (i) either by homogeneous catalysis through Fenton reaction using a carbonaceous cathode generating H_2O_2 and regenerating Fe^{2+} (Eqs. (1a)–(1d)) [12–15] combined with the addition of a catalytic amount of Fe^{2+} (< 0.2 mM) – unless initially present in solution [16], namely electro-Fenton (EF), and/or (ii) by heterogeneous catalysis through anodic oxidation (AO) in the presence of a high O_2 evolution overvoltage anode such as boron-doped diamond (BDD) (Eqs. (2a) and (2b)) [17–20].

$$O_2 + 2H^+ + 2e^- \rightarrow H_2O_2 \quad (1a)$$

$$Fe^{3+} + e^- \rightarrow Fe^{2+} \quad (1b)$$

$$Fe^{2+} + H_2O_2 \rightarrow Fe^{3+} + HO^- + {}^{\bullet}OH \quad (1c)$$

$${}^{\bullet}OH_{Fenton} + \text{compounds} \rightarrow \text{oxidation products} \quad (1d)$$

* Corresponding authors.
E-mail addresses: emmanuel.mousset@univ-lorraine.fr (E. Mousset), yoan.pechaud@u-pem.fr (Y. Pechaud).

https://doi.org/10.1016/j.apcatb.2018.08.055
Received 2 June 2018; Received in revised form 15 August 2018; Accepted 21 August 2018
Available online 29 August 2018
0926-3373/

Nomenclature

A	Surface area of anode (m^2)
a	Constant taking into account the dependency of K_L with [COD] (-)
b	Constant taking into account the dependency of K_L with [COD] (-)
$[COD]$	Chemical Oxygen Demand concentration at time t (mol m^{-3})
$[COD]_0$	Chemical Oxygen Demand concentration at time $t = 0$ (mol m^{-3})
F	Faraday constant (C mol^{-1})
I	Applied current intensity (A)
ICE_{anode}	Instantaneous current efficiency associated to the electro-oxidation at the anode surface (-)
$ICE_{cathode}$	Instantaneous current efficiency associated to the Fenton reaction involved from the reactions occurring at the cathode (-)
ICE_{exp}	Experimental instantaneous current efficiency (-)
ICE_{global}	Global instantaneous current efficiency (-)
$ICE_{global_{AO-BDD}}$	ICE_{global} for AO experiments with BDD anode (-)
$ICE_{global_{EF-BDD}}$	ICE_{global} for EF experiments with BDD anode (-)
ICE_{MO}	Instantaneous current efficiency associated to the mediated oxidation indirectly occurring from reactions at anode (-)
j_{appl}	Applied current density (A m^{-2})
j_{lim}	Limiting current density (A m^{-2})
K_L	Mass transfer coefficient at time t (m h^{-1})
K_{L0}	Mass transfer coefficient at time t = 0 (m h^{-1})
k_{abs}	Decay rate constant of the studied compound due to Fenton reaction (L $mmol^{-1}$ h^{-1})
k_{Fenton}	Observed (apparent) decay rate constant (h^{-1})
$k_{mediated}$	Apparent rate constant for organics decay by mediated oxidation (h^{-1})
k_{ox}	Decay rate constant of the studied compound due to mediated oxidation (L $mmol^{-1}$ h^{-1})
[$^{\bullet}$OH]	Concentration of $^{\bullet}$OH radical (mol m^{-3})
$[Ox]$	Concentration of oxidants (except $^{\bullet}$OH radical) (mol m^{-3})
r_{AO}	Rate of the reaction responsible for the degradation of organics at the anode surface by anodic oxidation with $^{\bullet}$OH (mol m^{-3} h^{-1})
r_{MO}	Reaction rate taking into account the mediated oxidation (mol m^{-3} h^{-1})
r_{Fenton}	Reaction rate taking into account the Fenton oxidation (mol m^{-3} h^{-1})
t	Electrolysis time (h)
t_{cr}	Critical time (h)
t_{A0}	Characteristic time of anodic oxidation (h)
t_{Fenton}	Characteristic time of Fenton oxidation (h)
$t_{mediated}$	Characteristic time of mediated oxidation (h)
V	Volume of treated solution (m^3)
y_i	Single numerically simulated value (-)
y_i'	Experimentally observed value (-)
y_M	Average of the numerically simulated values (-)

$$BDD + H_2O \rightarrow BDD(^{\bullet}OH_{AO}) + H^+ + e^- \quad (2a)$$

$$BDD(^{\bullet}OH_{AO}) + \text{compounds} \rightarrow BDD + \text{oxidation products} \quad (2b)$$

Thus, by combining EF and AO mechanisms this paired electrocatalysis process allows generating homogeneous $^{\bullet}$OH ($^{\bullet}OH_{Fenton}$) in the bulk solution and heterogeneous $^{\bullet}$OH ($^{\bullet}OH_{AO}$) at the anode surface. Thanks to the existence of two sites of radical production, the degradation and mineralization efficiencies of the EF process are very high [21–23], even with the most recalcitrant organic pollutants (> 95%) [8,24,25].

There is a critical lack of modeling studies focusing on EAOPs [9,26–30], though these models are of prime importance in the aim at predicting the kinetics of removal efficiency and for sizing the reactors for a further upscaling phase. Still, the contribution of $^{\bullet}OH_{AO}$, $^{\bullet}OH_{Fenton}$ and mediated oxidation (MO) in the degradation and mineralization efficiency has not been carried out and never been quantified. A better understanding of this contribution will guide in the selection on the kind of reactor design by optimizing either the heterogeneous or the homogeneous catalysis according to the main process involved. Moreover, the initial organic load is another important parameter that needs to be taken into account as it may influence the rate-determining step, i.e., either mass transport or charge transfer, and therefore the reactor design to be applied. In the early 2000s, Comninellis' group suggested a kinetic model that depicts the two phases observed during the compound and chemical oxygen demand (COD) decay [28]. A zero order model is noticed at the beginning of the treatment, i.e., when the concentration is still high, meaning that it is under current control, while at sufficiently low concentration it switches to mass transfer control leading to a first order model. However, this model does not take into account the MO that could occur in the bulk solution through intermediate oxidants other than $^{\bullet}$OH ($HOCl/ClO^-$, O_3, $SO_4^{\bullet-}$, etc.) [31–34] and need to be adapted for EF treatments. Moreover, the conventional instantaneous current efficiency (ICE) only takes into account the anode contribution [17,35] while it is necessary to define a current efficiency relation that could consider all the oxidation mechanisms involved.

In this context, this study proposes to bring new scientific insights through the three following objectives: (i) develop and validate a model that takes into account all the oxidation mechanisms (e.g., $^{\bullet}OH_{AO}$, $^{\bullet}OH_{Fenton}$ and MO) responsible for the degradation / mineralization efficiency of synthetic solution containing sulfate media at different initial organic load in an EF process with BDD anode, (ii) evaluate the contribution of each oxidation mechanism, and (iii) define a new adequate general current efficiency expression.

2. Mathematical modeling

A mathematical model has been developed in order to carry out the competitive mechanisms, i.e., charge transfer *vs* mass transport controls considering the involvement of several oxidation mechanisms.

2.1. Modelling software

The Aquasim® software was used to accomplish this model [36].

2.2. Assumptions

Some assumptions have been made to develop the mathematical model as listed below:

- The organic compounds can be degraded/mineralized by three ways: (i) at the surface of BDD anode by AO, (ii) in the bulk of electrolyte with $^{\bullet}$OH radical formed through Fenton reaction by EF and (iii) in the bulk of electrolyte and at anode vicinity through MO in presence of sulfate media ($SO_4^{\bullet}$, $S_2O_8^{2-}$, O_3, …),
- The quasi-steady state approximation (QSSA) hypothesis is considered for $^{\bullet}$OH and for MO [7,9,37],
- The batch electrochemical reactor is considered as perfectly mixed,
- The temperature and the volume of solution are considered constant.

2.3. Reaction rates and mass balance

The time at which the current density regime switch to the mass transfer control is called critical time (t_{cr}) and can be expressed as follow [38]:

$$t = t_{cr}\ at\ j_{appl} = j_{lim} \tag{3}$$

with $j_{appl} = \frac{I}{A}\ and\ j_{lim} = 4FK_L[COD]$

where j_{appl} is the applied current density (A m^{-2}), I is the applied current intensity (A), j_{lim} is the limiting current density (A m^{-2}) given at a COD concentration ([COD]) (mol m^{-3}) at time t, F is the Faraday constant (96 485 C mol^{-1}), K_L is the mass transfer coefficient (m h^{-1}), and A is the surface area of the BDD anode (2×10^{-4} m^2).

In AO-BDD experiments, the rate of the reaction responsible for the degradation of organics at the anode surface by AO (r_{AO}) from water discharge (Eqs. (2a) and (2b)) was adapted from the one given by previous authors [37–39] and was varying according to the t_{cr} value (Eqs. (4) and (5)).

$$if\ j_{appl} < j_{lim}\ then,\ r_{AO} = \frac{K_L A[COD]_0}{V} = K_{L_0}(1-a[COD]^b)\frac{A[COD]_0}{V} \tag{4}$$

$$if\ j_{appl} > j_{lim}\ then,\ r_{AO} = \frac{K_L A[COD]}{V} = K_{L_0}(1-a[COD]^b)\frac{A[COD]}{V} \tag{5}$$

Where K_L and K_{L_0} are the mass transfer coefficients at time t and time t = 0 respectively, while a and b constants take into account the dependency of K_L with [COD], $[COD]_0$ is the [COD] at time t = 0, and V is the volume of the treated solution (0.4×10^{-3} m^3).

Another reaction whose rate should be taken into account in AO-BDD experiments is the MO (r_{MO}) due to the formation of other oxidants (Ox) than $^{\bullet}OH_{AO}$ at the vicinity of the BDD surface (Eq. (6)). Though initially this kinetics equation is considered as second order, concentrations of oxidants ([Ox]) can be assumed to reach a pseudo-steady state value so that the final reaction order is one [37].

$$r_{MO} = k_{ox}[Ox][COD] = k_{mediated}[COD] \tag{6}$$

where k_{ox} is the decay rate constant of the studied compound due to MO ($m^3\ mol^{-1}\ h^{-1}$) and $k_{mediated}$ is the apparent rate constant (h^{-1}) for organics decay by MO.

In EF-BDD process, a third reaction rate was taken into account for the Fenton reaction in bulk solution (r_{Fenton}) (Eq. (7)), considering the QSSA for $^{\bullet}OH$ concentration ([$^{\bullet}OH$]) [7].

$$r_{Fenton} = k_{abs}[^{\bullet}OH][COD] = k_{Fenton}[COD] \tag{7}$$

where k_{abs} is the decay rate constant of the studied compound due to Fenton reaction ($m^3\ mol^{-1}\ h^{-1}$) and k_{Fenton} is the observed (apparent) decay rate constant (h^{-1}).

Thus, in the batch reactor the mass balance led to the following global reaction (Eq. (8)):

$$V\frac{dCOD}{dt} = -V\sum_i r_i \tag{8}$$

where r_i is the kinetic rate of oxidation process i; i represents the AO and MO in the case of AO-BDD experiments while i consists of the AO, MO and the Fenton oxidation in the case of EF-BDD experiments.

2.4. Global instantaneous current efficiency (ICE_{global})

A novel expression of the global instantaneous current efficiency (ICE_{global}), which represent the charge devoted to degrade and mineralize Tween 80 solution to the total charge passed during the electrolysis, has been proposed considering the three oxidation mechanisms involved in EF-BDD cells, i.e., AO, Fenton and MO processes, according to the following relation (Eq. (9)):

$$ICE_{global} = \frac{4FV}{I}.\frac{d[COD]}{dt} \tag{9}$$

From this expression, ICE_{global} has been separated into three parts in the model:

(i) ICE_{anode} associated to the electro-oxidation at the anode surface:

$$ICE_{anode} = \frac{4FV}{I}r_{AO} \tag{10}$$

- $ICE_{cathode}$ associated to the Fenton reaction occurring at the cathode (Eqs. (1a) and (1b)):

$$ICE_{cathode} = \frac{4FV}{I}r_{Fenton} \tag{11}$$

- ICE_{MO} associated to the MO indirectly occurring from reactions at anode:

$$ICE_{MO} = \frac{4FV}{I}r_{mediated} \tag{12}$$

From these three expressions, the ICE_{global} can be calculated as the sum of each ICE, depending on the kind of treatment:

$$ICE_{global_{AO-BDD}} = ICE_{anode} + ICE_{cathode} + ICE_{MO} \tag{13}$$

$$ICE_{global_{EF-BDD}} = ICE_{anode} + ICE_{cathode} + ICE_{MO} \tag{14}$$

where $ICE_{global_{AO-BDD}}$ is the ICE_{global} for AO experiments with BDD anode (AO-BDD) and $ICE_{global_{EF-BDD}}$ is the ICE_{global} for EF experiments with BDD anode (EF-BDD).

The experimental ICE has been calculated by the following expression:

$$ICE_{exp} = \frac{\frac{4FV}{I}([COD]_t - [COD]_{t+\Delta t})}{\Delta t} \tag{15}$$

where $[COD]_t$ and $[COD]_{t+\Delta t}$ are the CODs values at times t and $t+\Delta t$, respectively.

2.5. Model calibration

Calibration of the model was performed by adjusting unknown parameters until the model outputs adequately fit the experimental observations.

2.6. Model validation

Two methods were used for the comparison of model results with experimental measurements, the Modelling Efficiency (ME) (Eq. (16)) and the Index of Agreement (IoA) (Eq. (17)) [21,40]. Unknown parameters were calibrated by optimizing these two criteria.

$$ME = 1 - \frac{\sum_{i=1}^{K}(y_i - y_i')^2}{\sum_{i=1}^{K}(y_i - y_M)^2} \tag{16}$$

$$IoA = 1 - \frac{\sum_{i=1}^{K}(y_i - y_i')^2}{\sum_{i=1}^{K}(|y_i' - y_M| + |y_i - y_M|)^2} \tag{17}$$

where K is the number of observed values, y_i is the single numerically simulated value, y_i' is the corresponding experimentally observed value, y_M is the average of the numerically simulated values.

3. Experimental

3.1. Chemicals

All the following products were used at analytical grade without any further purification: methanol (HPLC grade), sodium sulphate and 2-(P-

toluidino)naphthalene-6-sulfonic acid sodium (TNS) and Tween 80 ($C_{64}H_{124}O_{26}$; 1310 g mol^{-1}) were purchased from Aldrich. Heptahydrated ferrous sulfate ($FeSO_4$•$7H_2O$), sulfuric acid and potassium dihydrogen phosphate (KH_2PO_4) were supplied by Acros. Potassium hydrogen phthalate ($C_8H_5KO_4$) from Nacalai Tesque was employed. Ultrapure water (UPW) from a Millipore Simplicity 185 (resistivity > 18 MΩ cm) system was used in all experiments.

3.2. Electrolysis experiments

EF experiments (EF-BDD) were performed in a 0.40 L undivided, open and cylindrical glass electrochemical reactor at current controlled conditions. The electrochemical cell was monitored by a power supply HAMEG 7042-5 by applying a constant current intensity of 1000 mA, corresponding to an average cell potential of 6.3 V. The cathode was a 150 cm^2 carbon-felt piece (Carbone-Lorraine). The anode studied was a BDD double side-coated on niobium (Nb) plate (20 cm^2 of immersed surface area) (Condias Gmbh, Germany) and was centered in the cell and surrounded by cathode which covered the inner wall of the cell, with an inter-electrode distance of 3 cm. The anode to volume ratio surface was 5 $m^2\ m^{-3}$. Sodium sulphate (0.150 M) was added as supporting electrolyte in the medium. $FeSO_4$•$7H_2O$ was also added at 0.2 mM as source of Fe^{2+} ion as catalyst. Prior to each experiment, the solutions were saturated in O_2 (8.53 mg $O_2\ L^{-1}$ at 22 °C) by supplying compressed air bubbling through the solution during 10 min before the beginning of the treatment. Solutions were stirred continuously and vigorously by a magnetic stirrer in order to supply dissolved O_2 at the cathode during the electrolysis. Also, the high cathode to volume ratio (38 $m^2\ m^{-3}$) was applied in order to increase the number of O_2 adsorption sites and facilitate its subsequent reduction into H_2O_2 (Eq. (1a)). The pH of initial solutions was set to the optimal value of 3.0 (± 0.1) by the addition of H_2SO_4 (1 M) solution. The pH changes were

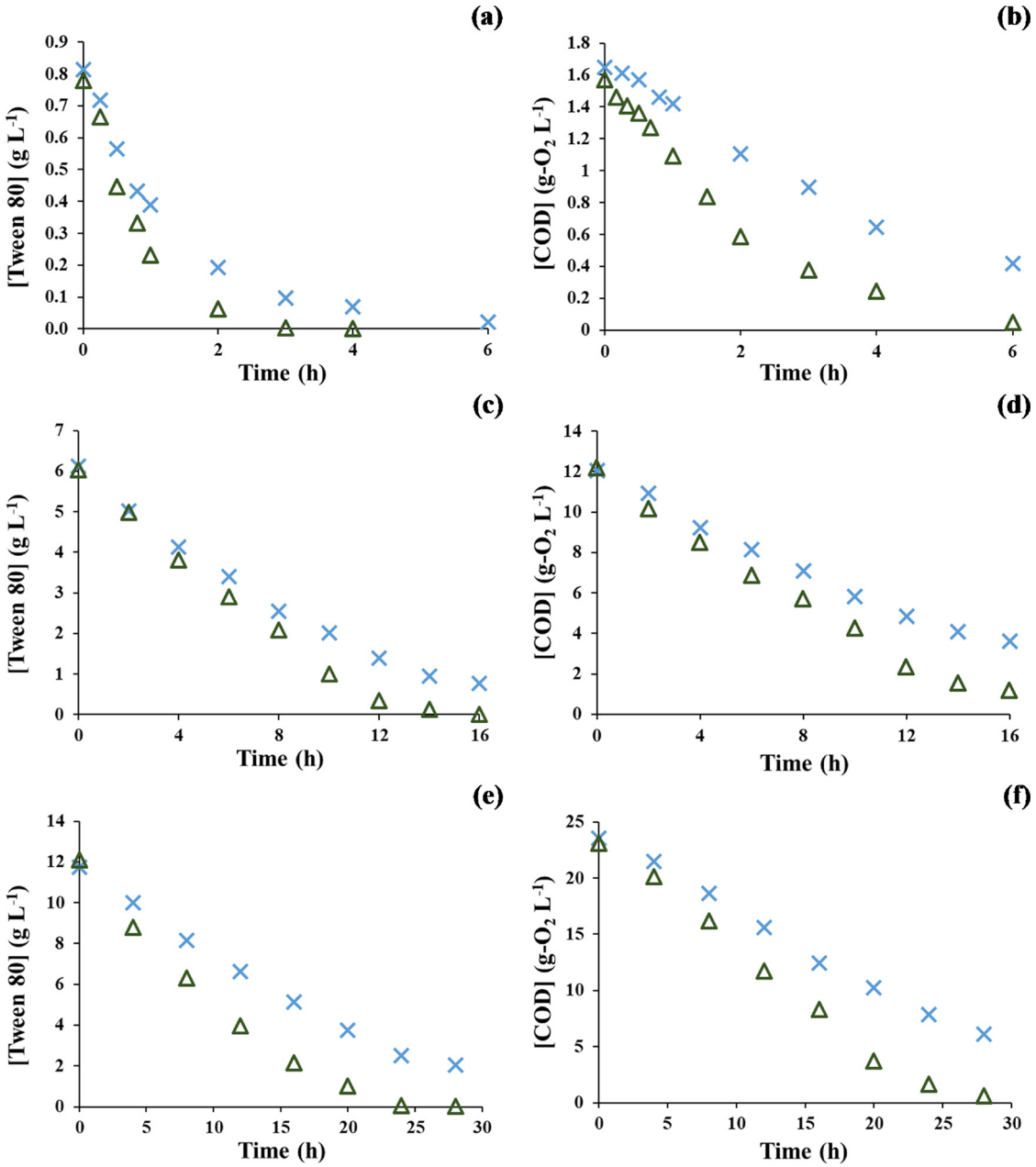

Fig. 1. Time course of Tween 80 ((a), (c), (e)) and COD ((b), (d), (f)) removal during AO-BDD (×) and EF-BDD (Δ) treatments at different initial Tween 80 ((a) 0.8 g L^{-1}, (c) 6.0 g L^{-1}, (e) 12.0 g L^{-1}) and COD concentrations ((b) 1.61 g-$O_2\ L^{-1}$, (d) 12.1 g-$O_2\ L^{-1}$, (f) 23.3 g-$O_2\ L^{-1}$). Operating conditions: I = 1 A, V = 0.4 L, [Na_2SO_4] = 150 mM, pH = 3 and [Fe^{2+}] = 0.2 mM (for EF treatments only).

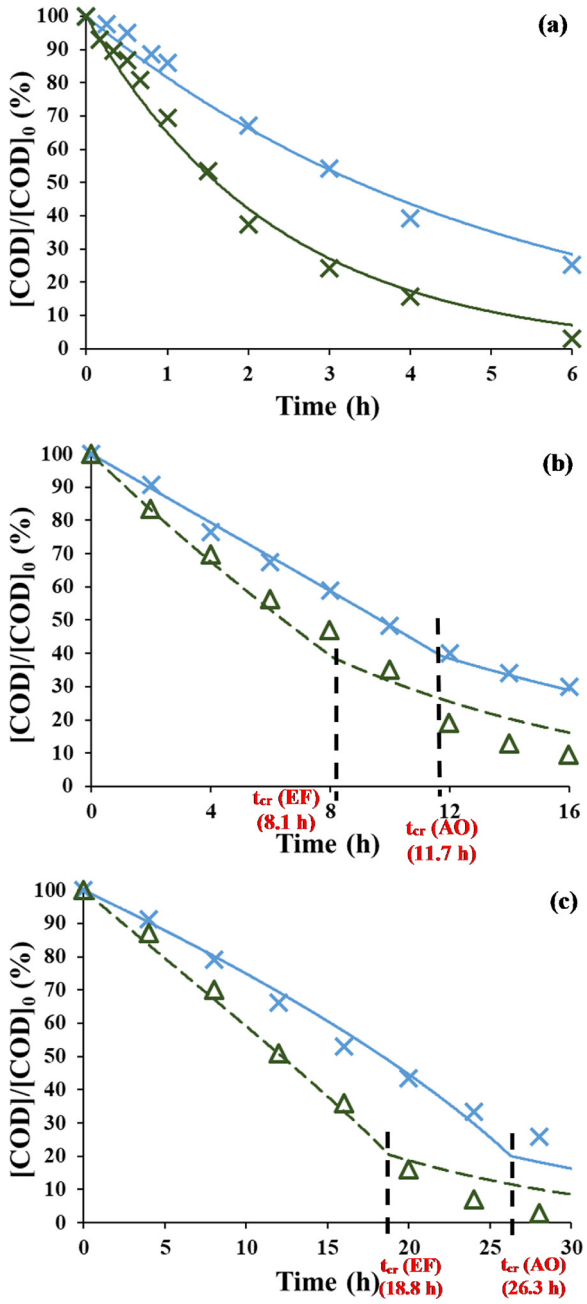

Fig. 2. Influence of initial COD concentration ((a) 1.61 g-O_2 L^{-1}, (b) 12.1 g-O_2 L^{-1}, and (c) 23.3 g-O_2 L^{-1}) on the kinetics of charge transfer control ($t < t_{cr}$) vs mass transport control ($t > t_{cr}$). AO-BDD (— / ×) and EF-BDD (– – – / Δ); model (— / – – –) and experimental data (markers (× / Δ)).

negligible during the electrolysis at pH 3.0; it decreased only to 2.8 (± 0.1) at the end of experiments. Different Tween 80 concentrations were monitored: 0.8, 6.0 and 12.0 g L^{-1}, corresponding to the following initial measured COD concentrations ($[COD]_0$): 1.61, 12.1 and 23.3 g-O_2 L^{-1}. Tween 80 is a surfactant that has been selected as model compound, since it is widely used in soil remediation systems [41–46]. Studying surfactant is also interesting as their viscosity raise when their concentration increase, which is a way to take into account the viscosity parameter in the developed model through the K_L expression in Eqs. (4) and (5). This model include the conditions when the compounds do not change the solution viscosity with electrolysis time.

AO experiments (AO-BDD) were performed in the same electrochemical cell and conditions than EF without adding $FeSO_4$•$7H_2O$. The same Tween 80 concentrations were carried out (0.8, 6 and 12 g L^{-1}).

3.3. Analytical procedures

The Tween 80 concentration was determined by a fluorimetric technique based on enhancement of the fluorescence intensity of TNS, when it is complexed with the surfactant [42]. This quantification method lead to errors in measurement ranging between 5% and 10% of the given values [42]. A Kontron SFM 25 spectrofluorimeter was set out at 318 nm for excitation and 428 nm for emission. All the measurements were done at constant temperature (22 °C ± 1). The protocol has been detailed in a previous study [42].

Chemical oxygen demand (COD) analyses were accomplished by a photometric method using a Spectroquant® NOVA 60 (Merck) equipment. The samples were diluted and prepared by adding 2 mL of each one in COD Cell test (15–300 mg O_2 L^{-1} range) (Merck) and by heating at 148 °C during two hours with a Spectroquant® TR 420 (Merck). The tubes were let cool to room temperature before analysis. The three Tween 80 initial solutions (0.8, 6 and 12 g L^{-1}) were corresponding to COD values of 1.61, 12.1 and 23.3 g-O_2 L^{-1}, respectively.

4. Results and discussions

4.1. Tween 80 and COD removal trends

The Tween 80 and COD decay have been monitored at three different initial COD concentrations of 1.61, 12.1 and 23.3 g-O_2 L^{-1}, considering two kinds of electrochemical treatments (AO-BDD and EF-BDD) and the experimental results are displayed in Fig. 1. The Tween 80 was quasi-completely degraded (> 99.9%) after 4 h, 16 h and 28 h with EF-BDD treatment of 0.8, 6 and 12 g L^{-1} solutions respectively, while the COD removal was 97%, 91% and 98% at these respective time. Contrastingly, after 4 h, 16 h and 28 h of AO-BDD treatment, the removal yields of Tween 80 were 92%, 87% and 82% respectively, corresponding to COD removal yields of 61%, 71% and 74%, respectively. Therefore, it can be observed that EF-BDD experiments depicts quicker kinetics than AO-BDD whatever the initial Tween 80 and COD concentrations. This is attributed to the two sources of $^{\bullet}OH$ formation in EF-BDD (Eqs. (1a) and (1d), (2a) and (2b)) as compared to one source in the case of AO-BDD (Eqs. (2a) and (2b)).

In addition, it was noticed that 75% of COD removal during EF-BDD treatment was reached after 3 h, 11 h and 18 h as the initial COD concentration increased while it was after 6 h, 16 h and 28 h with AO-BDD tests. This feature highlights the initial concentration dependency of the kinetics, depicting a different order of reaction than a pseudo-first order kinetic model as it is usually considered in such oxidative treatments [7,9]. Interestingly, the curves seem having different trends according to both the treatment time and the initial COD concentration. Previous authors, mainly Comninellis team [28], have shown that in the presence of BDD anode, two successive regimes could be observed depending on both the applied current density and the initial concentration of pollutants. A more recent study even proposed three consecutive regimes varying with the applied current density [47]. A mathematical model has been developed and compared with the experimental data to further understand this behavior in the following section 4.2.

4.2. Experimental data vs proposed model: charge transfer / mass transport competition

The mathematical model representing the COD removal yield against the treatment time is plotted in Fig. 2 and is compared with the experimental data. Firstly, it can be seen that ME and IoA values were close to 1, i.e. higher than 0.98 (except 0.968 with EF-BDD at medium concentration) and 0.99, respectively, as shown in Table 1. This confirms that the model could be validated by experimental data and thus emphasizes the importance of the reaction rates along with the coefficient values that have been considered.

Secondly, it was noticed that critical times were presents only for

Table 1
Validation of the model.

$[COD]_0$ (g-O_2 L^{-1})	Kind of process	ME	IoA
1.61	AO-BDD	0.9816	0.9958
	EF-BDD	0.9853	0.9966
12.1	AO-BDD	0.9970	0.9992
	EF-BDD	0.9680	0.9926
23.3	AO-BDD	0.9820	0.9952
	EF-BDD	0.9835	0.9962

the two highest COD concentration experiments. It means that at the lowest concentration j_{appl} was higher than j_{lim} all along the treatment as depicted in Fig. 3a and b. In this case, the pollutant was excessively diluted so that the charge transfer was faster than the mass transport being the rate limiting step. On the contrary, the experiments at higher initial COD concentration depicted a lower j compared to j_{lim} until 8.1 h and 11.7 h with EF-BDD and AO-BDD tests, respectively, at 12.1 g-O_2 L^{-1} as well as until 18.8 h and 26.3 h with EF-BDD and AO-BDD experiments, respectively, at 23.3 g-O_2 L^{-1} as highlighted in Fig. 3c–f. In these cases, the experiment is under current control, i.e., the charge transfer is the rate-determining step, at the beginning of the treatment while at sufficiently low concentration it switches to mass transfer control. It is further interesting to note that the t_{cr} where not the same for EF and AO experiments. In fact, t_{cr} depends on j_{lim} which depends on the COD concentration at time t. Since EF treatments lead to quicker degradation and mineralization as shown in section 4.1, t_{cr} values were lower in EF experiments. It is important to highlight that this constitutes a difference with the existing model that assume a t_{cr} dependent to the initial COD concentration [37–39,47], and therefore does not consider the COD removal rate. In the present study it seems that this assumption made by previous works cannot be certified. It further approve the inexistence - in our conditions - of the regime that depend on the limiting current density of direct transfer of electron, on the contrary to the suggestion made by Lan et al. [47] since no direct electro-oxidation was noticed in our experiments.

Moreover, there are other interesting distinction with the existing model such as the number of oxidation mechanisms and the mass

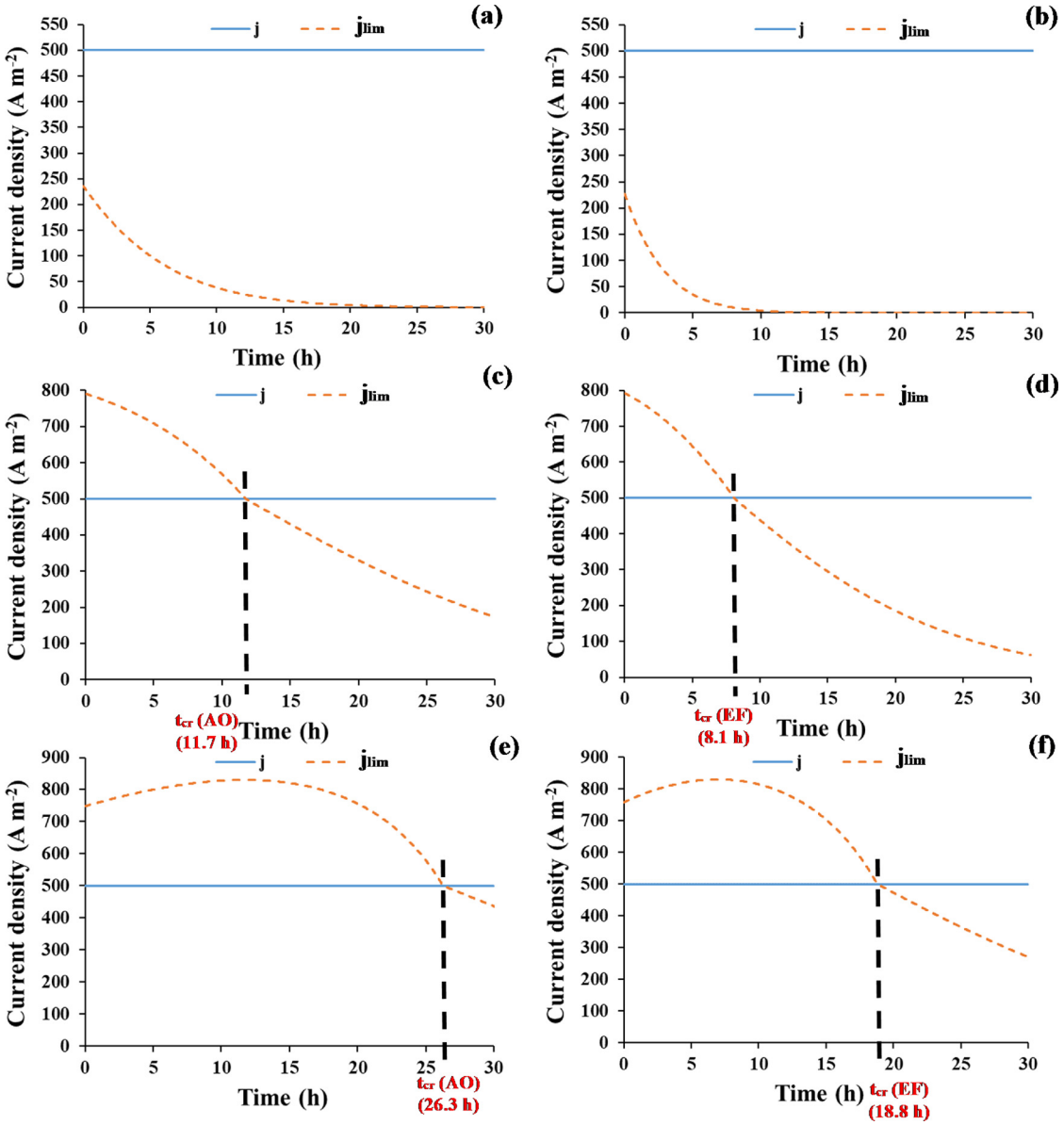

Fig. 3. Influence of initial COD concentration ((a, b) 1.61 g-O_2 L^{-1}, (c, d) 12.1 g-O_2 L^{-1}, and (e, f) 23.3 g-O_2 L^{-1}) on the kinetics of charge transfer control ($j < j_{lim}$) vs mass transport control ($j > j_{lim}$) during AO-BDD (a, c, e) or EF-BDD (b, d, f) experiments.

transfer coefficient expression that are taken into account. Those criteria and their contributions in EF / AO process efficiency are discussed in the following section 4.3.

4.3. Influence of parameters and oxidation mechanisms contribution

The values of the different parameters used in this model are represented in Table 2. The expression of K_L is modified compared to the literature. The influence of the concentration of surfactant on the mass transfer coefficient is introduced (Eqs. (4) and (5)). K_L was proposed to increase when the concentration decreases, considering two more coefficients - *a* and *b* - whose values equaled 0.239 and 0.200 respectively, which was close to the values given in literature in the presence of surfactant [48]. This relation illustrates that the presence of Tween 80 in water affects the mass transfer coefficient compared to water with a very low amount of Tween 80. The influence of Tween 80 on mass transfer coefficient could be ascribed to the higher viscosity of Tween 80 (1.00–1.14 mPa s [49]) as compared to studied compounds in literature [50–53]. Tween 80 being a surfactant, its concentration range has an impact to the solution viscosity as previously demonstrated [49] and could explain the decrease of the K_L value with Tween 80 concentration. A K_{L_0} value of 6.9×10^{-6} m s^{-1} has been considered in the model, which is lower than the range of values given in literature ($1–7 \times 10^{-5}$ m s^{-1}) [37,54]. It could be ascribed to the different hydrodynamic conditions in our batch reactor - no bubbling and larger diameter of reactor - and to the fact that Tween 80 is a larger molecule with much higher molar weight (1310 g mol^{-1}) compared to compounds generally considered in literature (50-300 g mol^{-1}) [50–53]. Interestingly, it makes the global order of reaction more complex than a simple zero order (linear decrease) or first order (exponential decrease) model as usually described in literature [37–39,47]. It further strengthens the fact that K_L is a determining parameter to consider in order to accurately predicting the evolution of COD concentration in the electrochemical reactors.

The estimation of $k_{mediated}$ and k_{Fenton} values have been performed in the following way. In the AO-BDD experiments, MO process and AO process occur simultaneously. The rate of AO process has been estimated directly by Eqs. (4) and (5). From the experimental results on AO, the values of $k_{mediated}$ for the different initial concentrations have been estimated. For the EF-BDD experiments, $k_{mediated}$ values were kept at the same values than for AO-BDD experiments performed with a similar initial concentration. For EF-BDD, in addition to AO and MO, EF process occurs at the cathode. Thus the only one parameter to fix was k_{Fenton}. This parameter was estimated by adjusting the model to experimental results.

In the present model, a distinction between anodic oxidation, MO and Fenton oxidation - the later only for EF-BDD cells - has been introduced for the first time. In the aim at evaluating the order of magnitude on how quick the reaction is occurring, the characteristic times have been estimated and the expression for each process is given in Table 3 and they have been plotted in Fig. 4. In the case of Fenton and mediated oxidation the characteristic times are defined as the inverse of the respective pseudo-first order kinetic rate constant. It is important to highlight that in both cases, the characteristic times are assumed constant throughout the electrolysis as it is considered most of the time [9]. Whatever the initial concentration for AO-BDD experiments, the characteristic time of anodic oxidation, t_{AO}, decreases over time (Fig. 4a, c and e). This decrease is associated to the decrease of the mass transfer resistance with the decrease of the COD concentration. In other words, due to a decrease of Tween 80 concentration leading to a decrease of the apparent viscosity of the solution and in turn to an increase of the mass transfer parameter K_L. This is specific to the degradation of viscous solution. For the lower initial concentration, t_{AO} remains higher than $t_{mediated}$ meaning that MO process is faster than AO and thus the main process governing the COD removal is the MO for AO-BDD for this condition. For the two higher initial concentrations, t_{AO} is higher than $t_{mediated}$ during the first hours of treatment. After several hours the curves of the two characteristic times intersect and AO become the main process responsible for COD removal.

For EF-BDD experiments, the model predicts that t_{Fenton} is initially lower than $t_{mediated}$ and t_{AO} meaning that Fenton oxidation is the main process during the initial phase (Fig. 4b, d and f). Whatever the initial conditions, t_{Fenton} is lower than $t_{mediated}$ meaning that the kinetic of Fenton process is higher than mediated process. Two main reasons can explain this trend. Firstly, the oxidation power of hydroxyl radicals produced by Fenton reaction is higher than those oxidants generated at anode surface (O_3, $SO_4^{\bullet -}$, etc) to perform mediated oxidation. Secondly, the $^{\bullet}OH$ were produced at sufficiently high amount as compared to other oxidants, making Fenton the predominant oxidation mechanism in bulk solution.

In the same way as in AO-BDD cells, AO process becomes the main process involved in COD removal for the two higher initial concentrations experiments ($t_{A0} < t_{Fenton} < t_{mediated}$) after several hours, due to the decrease of the COD and thus of the mass transport resistance. It could also be attributed to the fact that with electrolysis time the generated intermediates are less reactive with $^{\bullet}OH$ radicals and therefore the contribution of electro-oxidation at BDD anode start being important in the degradation/mineralization mechanisms in parallel to $^{\bullet}OH$ oxidation.

4.4. Introducing the influence of Fenton oxidation and mediated oxidation in the ICE expression

In existing models, *ICE* is only defined based on the AO process involving BDD anode [38,39,55]. In this existing model, *ICE* is equal to 1 during the current control stage ($j_{appl} < j_{lim}$) followed by a subsequent exponential decrease with the electrolysis time when the system is under mass transport control ($j_{appl} > j_{lim}$). However, ICE_{exp} values higher than 1 were noticed in the present study for the medium and high concentrations experiments as depicted in Fig. 5 whatever the kind of treatment (EF-BDD or AO-BDD). Moreover, these ICE_{exp} values were evolving even during the current control phase. This is attributed to the additional MO mechanism in AO-BDD tests and to the supplementary MO and Fenton oxidation mechanisms in EF-BDD experiments as discussed in sub-section 4.3. Both mechanisms have not been considered in the previous modeling works. Therefore, it is proposed for the first time to introduce these mechanisms in the ICE_{global} expression, i.e., AO and MO in AO-BDD cells (Eq. (13)) and AO, MO and Fenton oxidation in EF-BDD cells (Eq. (14)).

The comparison between the simulated data and experimental results are illustrated in Fig. 5. Even if it is not fitting completely for high concentration experiments, the trends could be still observed, especially for EF-BDD cells. It is interesting to note that this suggested model allowed predicting the increase or decrease of *ICE* values even during the current control regime. The increase of *ICE* values at high concentration experiment is due to the MO mechanism that participate to additional COD removal as compared to the theoretical COD calculation based on

Table 2
Parameters used in the model.

Parameter	$[COD]_0$ (g-O_2 L^{-1})	Kind of process	Value
K_{L_0}	1.61 / 12.1 / 23.3	AO-BDD / EF-BDD	6.9×10^{-6} m s^{-1}
a	1.61 / 12.1 / 23.3	AO-BDD / EF-BDD	0.239
b	1.61 / 12.1 / 23.3	AO-BDD / EF-BDD	0.200
$k_{mediated}$	1.61	AO-BDD / EF-BDD	0.143 h^{-1}
	12.1	AO-BDD / EF-BDD	0.0248 h^{-1}
	23.3	AO-BDD / EF-BDD	0.0103 h^{-1}
k_{Fenton}	1.61	EF-BDD	0.223 h^{-1}
	12.1	EF-BDD	0.0353 h^{-1}
	23.3	EF-BDD	0.0176 h^{-1}

Table 3
Characteristic times of the processes.

Process	Characteristic time (h)
Anodic oxidation	$t_{AO} = \frac{V}{K_{L_0}\,(1 - a[COD]^b).A}$
Fenton oxidation	$t_{Fenton} = \frac{1}{k_{Fenton}}$
Mediated oxidation	$t_{mediated} = \frac{1}{k_{mediated}}$

the applied current (Eq. (15)). The decrease of *ICE* values is due to parasitic reaction such as oxidation of H_2O into O_2 and reduction of H^+ into H_2 that occurs increasingly with the electrolysis time.

Thus, this model is a first attempt to predict the *ICE* evolution during electrolysis subjected to several oxidation mechanisms occurred during EF process.

5. Conclusions

This work presents the influence of the initial COD concentration on the mass transport *vs* charge transfer during AO and EF treatments with BDD anode. A mathematical model considering three reaction rates has been validated with experimental data, considering the dependency of the mass transport coefficient with the concentration of the targeted pollutant (e.g. surfactant). This later feature highlights the importance of the viscosity in such type of effluent. A further interesting outcome is the heterogeneous catalysis (e.g. AO process) that has a primordial role in the degradation and mineralization of the solution at higher initial organic load after a certain treatment time before reaching the t_{cr}, while homogeneous catalysis (e.g. EF process) mechanism dominated at low COD concentration. Eventually, a novel *ICE* expression has been suggested based on the same model in order to take into account the three oxidation mechanisms involved. The *ICE* relation has been validated by experimental data and confirms again the important predicting role of the present model. This model could be enlarged to other kinds of electrochemical treatments that involve both heterogeneous and homogeneous oxidations in electrolysis treatment. Knowing the main

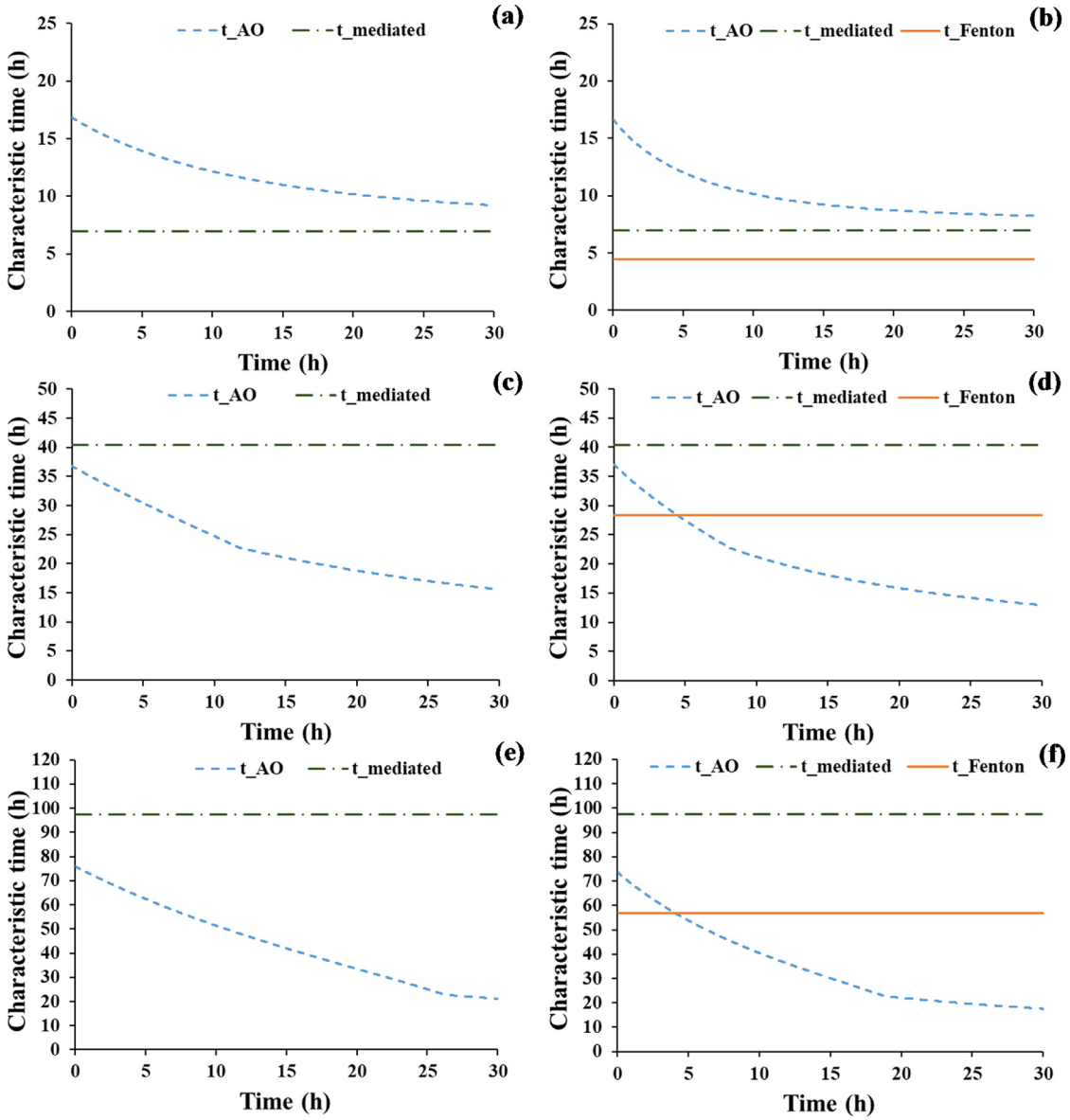

Fig. 4. Competition between the different characteristic times of the processes involved as a function of the treatment time of AO-BDD (a, c, e) or EF-BDD (b, d, f) experiments, at different initial COD concentrations ((a, b) 1.61 g-O_2 L^{-1}, (c, d) 12.1 g-O_2 L^{-1}, and (e, f) 23.3 g-O_2 L^{-1}).

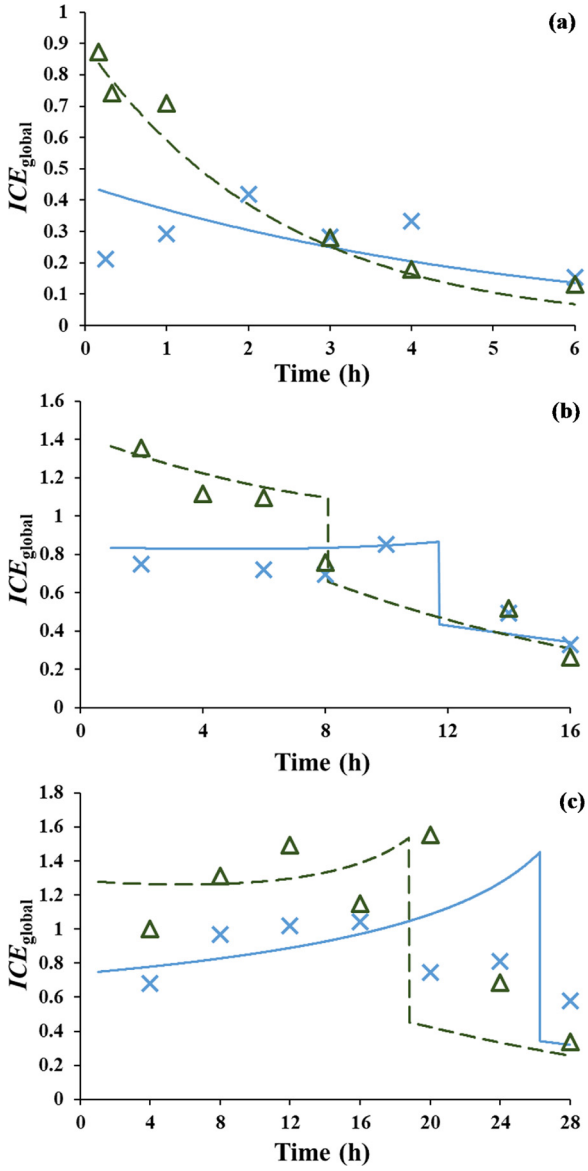

Fig. 5. Global instantaneous current efficiency (ICE_{global}) at different initial concentrations: (a) 1.61 g-O_2 L^{-1}, (b) 12.1 g-O_2 L^{-1}, and (c) 23.3 g-O_2 L^{-1}). AO-BDD (— / ×) and EF-BDD (– – – / Δ); model (— / – – –) and experimental data (markers (× / Δ)).

process involves and predicting their relative impact on the oxidation efficiency give promising perspectives in the reactor design optimization, a necessary step for the upscaling stage.

References

[1] S.D. Richardson, S.Y. Kimura, Water analysis: emerging contaminants and current issues, Anal. Chem. 88 (2016) 546–582.

[2] T. Basile, A. Petrella, M. Petrella, G. Boghetich, V. Petruzzelli, S. Colasuonno, D. Petruzzelli, Review of endocrine-disrupting-compound removal technologies in water and wastewater treatment plants: an EU perspective, Ind. Eng. Chem. Res. 50 (2011) 8389–8401.

[3] S. Rodriguez, A. Santos, A. Romero, Effectiveness of AOP's on abatement of emerging pollutants and their oxidation intermediates: nicotine removal with Fenton's reagent, Desalination 280 (2011) 108–113.

[4] S. Esplugas, D.M. Bila, L.G.T. Krause, M. Dezotti, Ozonation and advanced oxidation technologies to remove endocrine disrupting chemicals (EDCs) and pharmaceuticals and personal care products (PPCPs) in water effluents, J. Hazard. Mater. 149 (2007) 631–642.

[5] M.A. Oturan, J.-J. Aaron, Advanced oxidation processes in water/wastewater treatment: principles and applications. A review, Crit. Rev. Environ. Sci. Technol. 44 (2014) 2577–2641.

[6] I. Oller, S. Malato, J.A. Sánchez-Pérez, Combination of Advanced Oxidation Processes and biological treatments for wastewater decontamination-A review, Sci. Total Environ. 409 (2011) 4141–4166.

[7] E. Brillas, I. Sirés, M.A. Oturan, Electro-Fenton process and related electrochemical technologies based on Fenton's reaction chemistry, Chem. Rev. 109 (2009) 6570–6631.

[8] E. Mousset, N. Oturan, M.A. Oturan, An unprecedented route of OH radical reactivity evidenced by an electrocatalytical process: ipso-substitution with perhalogenocarbon compounds, Appl. Catal. B: Environ. 226 (2018) 135–146.

[9] E. Mousset, L. Frunzo, G. Esposito, E.D. van Hullebusch, N. Oturan, M.A. Oturan, A complete phenol oxidation pathway obtained during electro-Fenton treatment and validated by a kinetic model study, Appl. Catal. B: Environ. 180 (2016) 189–198.

[10] I. Sirés, E. Brillas, M.A. Oturan, M.A. Rodrigo, M. Panizza, Electrochemical advanced oxidation processes: today and tomorrow. A review, Environ. Sci. Pollut. Res. Int. 21 (2014) 8336–8367.

[11] B.P. Chaplin, Critical review of electrochemical advanced oxidation processes for water treatment applications, Environ. Sci. Process. Impacts 16 (2014) 1182–1203.

[12] L. Zhou, M. Zhou, Z. Hu, Z. Bi, K.G. Serrano, Chemically modified graphite felt as an efficient cathode in electro-Fenton for p-nitrophenol degradation, Electrochim. Acta 140 (2014) 376–383.

[13] E. Mousset, Z. Wang, J. Hammaker, O. Lefebvre, Electrocatalytic phenol degradation by a novel nanostructured carbon fiber brush cathode coated with graphene ink, Electrochim. Acta 258 (2017) 607–617.

[14] E. Mousset, V. Huang Weiqi, B. Foong Yang Kai, J.S. Koh, J.W. Tng, Z. Wang, O. Lefebvre, A new 3D-printed photoelectrocatalytic reactor combining the benefits of a transparent electrode and the Fenton reaction for advanced wastewater treatment, J. Mater. Chem. A Mater. Energy Sustain. 5 (2017) 24951–24964.

[15] W. Yang, M. Zhou, J. Cai, L. Liang, G. Ren, L. Jiang, Ultrahigh yield of hydrogen peroxide on graphite felt cathode modified with electrochemically exfoliated graphene, J. Mater. Chem. A Mater. Energy Sustain. 00 (2017) 1–11.

[16] E. Mousset, D. Huguenot, E.D. Van Hullebusch, N. Oturan, G. Guibaud, G. Esposito, M.A. Oturan, Impact of electrochemical treatment of soil washing solution on PAH degradation efficiency and soil respirometry, Environ. Pollut. 211 (2016) 354–362.

[17] M. Panizza, G. Cerisola, Direct and mediated anodic oxidation of organic pollutants, Chem. Rev. 109 (2009) 6541–6569.

[18] C.A. Martinez-Huitle, M.A. Rodrigo, I. Sires, O. Scialdone, Single and coupled electrochemical processes and reactors for the abatement of organic water pollutants: A critical review, Chem. Rev. 115 (2015) 13362–13407.

[19] M.A. Rodrigo, N. Oturan, M.A. Oturan, Electrochemically assisted remediation of pesticides in soils and water: a review, Chem. Rev. 114 (2014) 8720–8745.

[20] L. Gherardini, P.A. Michaud, M. Panizza, C. Comninellis, N. Vatistas, Electrochemical oxidation of 4-chlorophenol for wastewater treatment: definition of normalized current efficiency (φ), J. Electrochem. Soc. 148 (2001) D78–D82.

[21] C. Trellu, Y. Péchaud, N. Oturan, E. Mousset, D. Huguenot, E.D. van Hullebusch, G. Esposito, M.A. Oturan, Comparative study on the removal of humic acids from drinking water by anodic oxidation and electro-Fenton processes: mineralization efficiency and modelling, Appl. Catal. B: Environ. 194 (2016) 32–41.

[22] F.C. Moreira, R.A.R. Boaventura, E. Brillas, V.J.P. Vilar, Electrochemical advanced oxidation processes: a review on their application to synthetic and real wastewaters, Appl. Catal. B: Environ. 202 (2017) 217–261.

[23] I. Sirés, E. Brillas, Remediation of water pollution caused by pharmaceutical residues based on electrochemical separation and degradation technologies: a review, Environ. Int. 40 (2012) 212–229.

[24] N. Oturan, E. Brillas, M.A. Oturan, Unprecedented total mineralization of atrazine and cyanuric acid by anodic oxidation and electro-Fenton with a boron-doped diamond anode, Environ. Chem. Lett. 10 (2012) 165–170.

[25] E. Brillas, C.A. Martínez-Huitle, Decontamination of wastewaters containing synthetic organic dyes by electrochemical methods. An updated review, Appl. Catal. B: Environ. 166–167 (2015) 603–643.

[26] M.T. Fukunaga, J.R. Guimarães, R. Bertazzoli, Kinetics of the oxidation of formaldehyde in a flow electrochemical reactor with TiO_2/RuO_2 anode, Chem. Eng. J. 136 (2008) 236–241.

[27] H. Liu, X.Z. Li, Y.J. Leng, C. Wang, Kinetic modeling of electro-Fenton reaction in aqueous solution, Water Res. 41 (2007) 1161–1167.

[28] M. Panizza, P.A. Michaud, G. Cerisola, C. Comninellis, Anodic oxidation of 2-naphthol at boron-doped diamond electrodes, J. Electroanal. Chem. Lausanne (Lausanne) 507 (2001) 206–214.

[29] M. Panizza, P.A. Michaud, G. Cerisola, C. Comninellis, Electrochemical treatment of wastewaters containing organic pollutants on boron-doped diamond electrodes : prediction of specific energy consumption and required electrode area, Electrochem. Commun. 3 (2001) 336–339.

[30] S. Qiu, D. He, J. Ma, T. Liu, T.D. Waite, Kinetic modeling of the electro-Fenton process: quantification of reactive oxygen species generation, Electrochim. Acta 176 (2015) 51–58.

[31] C.A. Martínez-Huitle, E. Brillas, Electrochemical alternatives for drinking water disinfection, Angew. Chem. Int. Ed. Engl. 47 (2008) 1998–2005.

[32] E. Mousset, S. Pontvianne, M.-N. Pons, Fate of inorganic nitrogen species under homogeneous Fenton combined with electro-oxidation/reduction treatments in synthetic solutions and reclaimed municipal wastewater, Chemosphere 201 (2018) 6–12.

[33] C.D.N. Brito, D.M. de Araújo, C.A. Martínez-Huitle, M.A. Rodrigo, Understanding active chlorine species production using boron doped diamond films with lower and higher sp^3/sp^2 ratio, Electrochem. Commun. 55 (2015) 34–38.

[34] K. Serrano, P.A. Michaud, C. Comninellis, A. Savall, Electrochemical preparation of peroxodisulfuric acid using boron-doped diamond thin film electrodes, Electrochim. Acta 48 (2002) 431–436.

[35] C. Comninellis, C. Pulgarin, Anodic oxidation of phenol for wastewater treatment, J. Appl. Electrochem. 21 (1991) 703–708.
[36] P. Reichert, Computer Program for the Identication and Simulation of Aquatic Systems, (1998).
[37] F. Sopaj, M.A. Rodrigo, N. Oturan, F.I. Podvorica, J. Pinson, M.A. Oturan, Influence of the anode materials on the electrochemical oxidation efficiency. Application to oxidative degradation of the pharmaceutical amoxicillin, Chem. Eng. J. 262 (2015) 286–294.
[38] P.-A. Michaud, C. Comninellis, Comportement anodique du diamant synthétique dopé au bore, PhD thesis, EPFL, Switzerland, 2002.
[39] M. Panizza, P.A. Michaud, G. Cerisola, C. Comninellis, Anodic oxidation of 2-naphthol at boron-doped diamond electrodes, J. Electroanal. Chem. Lausanne (Lausanne) 507 (2001) 0206–0214.
[40] E. Mousset, Z. Wang, J. Hammaker, O. Lefebvre, Physico-chemical properties of pristine graphene and its performance as electrode material for electro-Fenton treatment of wastewater, Electrochim. Acta 214 (2016) 217–230.
[41] E. Mousset, N. Oturan, E.D. van Hullebusch, G. Guibaud, G. Esposito, M.A. Oturan, Influence of solubilizing agents (cyclodextrin or surfactant) on phenanthrene degradation by electro-Fenton process - Study of soil washing recycling possibilities and environmental impact, Water Res. 48 (2014) 306–316.
[42] E. Mousset, N. Oturan, E.D. van Hullebusch, G. Guibaud, G. Esposito, M.A. Oturan, A new micelle-based method to quantify the Tween 80® surfactant for soil remediation, Agron. Sustain. Dev. 33 (2013) 839–846.
[43] E. Mousset, C. Trellu, N. Oturan, M.A. Oturan, Soil remediation by electro-Fenton process, in: M. Zhou, I. Sires, M.A. Oturan (Eds.), The Handbook of Environmental Chemistry, Springer, 2018, pp. 399–423.
[44] J. Gómez, M.T. Alcántara, M. Pazos, M.A. Sanromán, Remediation of polluted soil by a two-stage treatment system: desorption of phenanthrene in soil and electrochemical treatment to recover the extraction agent, J. Hazard. Mater. 173 (2010) 794–798.
[45] S. Paria, Surfactant-enhanced remediation of organic contaminated soil and water, Adv. Colloid Interface Sci. 138 (2008) 24–58.
[46] C. Trellu, E. Mousset, Y. Pechaud, D. Huguenot, E.D. van Hullebusch, G. Esposito, M.A. Oturan, Removal of hydrophobic organic pollutants from soil washing/flushing solutions: a critical review, J. Hazard. Mater. 306 (2016) 149–174.
[47] Y. Lan, C. Coetsier, C. Causser, K. Groenen Serrano, An experimental and modelling study of the electrochemical oxidation of pharmaceuticals using a boron-doped diamond anode, Chem. Eng. J. 333 (2017) 486–494.
[48] M. Jamnongwong, K. Loubiere, N. Dietrich, G. Hébrard, Experimental study of oxygen diffusion coefficients in clean water containing salt, glucose or surfactant: consequences on the liquid-side mass transfer coefficients, Chem. Eng. J. 165 (2010) 758–768.
[49] K. Szymczyk, A. Taraba, Aggregation behavior of Triton X-114 and Tween 80 at various temperatures and concentrations studied by density and viscosity measurements, J. Therm. Anal. Calorim. 126 (2016) 315–326.
[50] X. Florenza, A.M.S. Solano, F. Centellas, C.A. Martínez-Huitle, E. Brillas, S. Garcia-Segura, Degradation of the azo dye Acid Red 1 by anodic oxidation and indirect electrochemical processes based on Fenton's reaction chemistry. Relationship between decolorization, mineralization and products, Electrochim. Acta 142 (2014) 276–288.
[51] A.R.F. Pipi, A.R. De Andrade, E. Brillas, I. Sirés, Total removal of alachlor from water by electrochemical processes, Sep. Purif. Technol. 132 (2014) 674–683.
[52] X. Yu, M. Zhou, Y. Hu, K. Groenen Serrano, F. Yu, Recent updates on electrochemical degradation of bio-refractory organic pollutants using BDD anode: a mini review, Environ. Sci. Pollut. Res. 21 (2014) 8417–8431.
[53] F.L. Souza, J.M. Aquino, K. Irikura, D.W. Miwa, M.A. Rodrigo, A.J. Motheo, Electrochemical degradation of the dimethyl phthalate ester on a fluoride-doped Ti/β-PbO_2 anode, Chemosphere 109 (2014) 187–194.
[54] A.M. Polcaro, A. Vacca, M. Mascia, S. Palmas, R. Pompei, S. Laconi, Characterization of a stirred tank electrochemical cell for water disinfection processes, Electrochim. Acta 52 (2007) 2595–2602.
[55] A. Kapałka, G. Fóti, C. Comninellis, Kinetic modelling of the electrochemical mineralization of organic pollutants for wastewater treatment, J. Appl. Electrochem. 38 (2008) 7–16.